Article ID: 1000-7032(2023)12-2128-08

Triple-activator Photoluminescence of Eu/Tb/SnO_2 Nanocrystals Co-doped Silica Glasses for Self-referencing Optical Temperature Measurement

CHEN Ping[1], GAO Yanpeng[1], HE Yong[1], DAI Nengli[2*]

(1. *School of Materials Science and Engineering, Hefei University of Technology, Hefei* 230009, *China*;
2. *Wuhan National Laboratory for Optoelectronics, Huazhong University of Science and Technology, Wuhan* 430074, *China*)

* *Corresponding Author, E-mail: dainl@mail. hust. edu. cn*

Abstract: Self-referencing optical thermometers have shown competitive advantages on fast response and high accuracy as they can avoid inevitable external factors like concentration change, excitation fluctuation, and detector loss. Herein, we report the triple-emitting photoluminescence of Eu/Tb/SnO_2 nanocrystals co-doped silica glasses. The temperature-dependent fluorescence intensity ratio of non-thermal coupled levels of Eu^{3+}($^5D_0$-$^7F_2$ transition, 620 nm)/Eu^{2+}($4f^65d$-$^8S_{7/2}$ transition, 434 nm) and Eu^{3+}($^5D_0$-$^7F_2$ transition, 620 nm)/Tb^{3+}($^5D_4$-$^7F_5$ transition, 542 nm) can be used for self-referencing temperature probing in a wide range of 298-773 K. The maximum relative thermal sensitivity S_r values can reach 2.3%·K^{-1} at 773 K, which is higher than most Eu/Tb co-doped materials. This work will contribute a new Eu/Tb co-doped material to self-referencing optical temperature measurement with triple activators.

Key words: rare earth ions; SnO_2 nanocrystals; photoluminescence; temperature measurement; silica glasses
CLC number: O482.31 **Document code**: A **DOI**: 10.37188/CJL.20230212

基于 Eu/Tb/SnO_2纳米晶体共掺杂二氧化硅玻璃的三激活剂光致发光自参考光学温度测量

陈 萍[1], 高延鹏[1], 何 勇[1], 戴能利[2*]

(1. 合肥工业大学 材料科学与工程学院, 安徽 合肥 230009;
2. 华中科技大学 武汉光电国家研究中心, 湖北 武汉 430074)

摘要: 自参考光学温度计在快速响应和高精度方面显示出竞争优势,因为可以规避一些不可避免的外部因素,如浓度变化、激发波动和检测器损耗。本文报道了 Eu/Tb/SnO_2纳米晶体共掺杂二氧化硅玻璃的三激活剂光致发光。基于 Eu^{3+}($^5D_0$-$^7F_2$跃迁,620 nm)/Eu^{2+}($4f^65d$-$^8S_{7/2}$跃迁,434 nm)和 Eu^{3+}($^5D_0$-$^7F_2$跃迁,620 nm)/Tb^{3+}($^5D_4$-$^7F_5$跃迁,542 nm)的非热耦合能级的温度依赖性荧光强度比可用于 298 ~ 773 K 宽范围内的自参考温度探测。在 773 K 时,最大相对热灵敏度 S_r可达 2.3%·K^{-1},高于大多数 Eu/Tb 共掺杂材料。这项工作将为三重激活剂的自参考光学温度测量提供一种新的 Eu/Tb 共掺杂材料。

关 键 词: 稀土离子; SnO_2 纳米晶; 光致发光; 温度测量; 二氧化硅玻璃

收稿日期: 2023-09-15; **修订日期**: 2023-10-02
基金项目: 国家自然科学基金(22101090); 中央高校基本科研业务费专项资金(JZ2023HGTB0224)
Supported by National Natural Science Foundation of China(22101090); Fundamental Research Funds for The Central Universities(JZ2023HGTB0224)

1 Introduction

As a fundamental thermodynamic parameter, temperature is highly essential in both science researches and industry applications. Considerable efforts have been put into temperature measurement[1-4]. Among numerous methods for measuring temperature, luminescence-based measurements have aroused interests of researchers because they have merits of quick response, precise resolution, contactless and noninvasive operation[5-7]. All these merits make it possible for measuring temperature in some extremely harsh environments based on fluorescence peak shift, bandwidth, intensity, and lifetime[8-11].

Generally, optical temperature probe includes two basic means by monitoring the temperature-induced changes of single emission or relative emission. Single emission detecting has the drawbacks of dependence on concentrations, pumping power, and some other experimental conditions. Relative emission method is based on different luminescent centers or different energy levels of one luminescent center, which can overcome the shortcomings of single emission method due to its independence on experimental fluctuations[12-15]. Specially, self-referencing optical temperature sensing based on fluorescence intensity ratio (FIR) of rare earth ions (RE) has been widely used for precise temperature sensing, which is one of relative emission method[5,16-18].

Usually, FIR methods are based on two thermal coupled levels (TCL) of RE[9]. The energy gap of TCL is 200−2 000 cm^{-1}, such as $^2H_{11/2}$ and $^4S_{3/2}$ level of Er^{3+}[9,19]. However, researches have shown that the higher sensitivity of FIR thermometer benefits from a larger energy gap[19-20]. Therefore, the sensitivity is restricted by the small energy gap of TCL. Besides, a small energy gap can lead to inferior signal discriminability due to the overlap of the two fluorescence peaks[21]. In addition, the energy level gap of most RE are non-thermal coupled levels (NTCL), especially for materials doped with more than one RE activator. However, FIR methods based on NTCL have been scarcely studied[9,19,22-23].

Eu/Tb co-doped materials have been widely used for FIR-type temperature measurement due to their distinguished red emission of Eu^{3+} ($^5D_0$-$^7F_2$ transition) and green emission of Tb^{3+} ($^5D_4$-$^7F_5$ transition)[8,14,16,24-26]. In this work, we reported Eu/Tb/SnO_2 nanocrystals (NCs) co-doped silica glasses for temperature sensing based on NTCL. The hybrid material was synthesized with the same method of our previous work[27-30]. Other than most Eu/Tb co-doped materials, the hybrid here shows not only the characteristic emissions of Eu^{3+} and Tb^{3+}, but also the blue emission of Eu^{2+} ($4f^65d$-$^8S_{7/2}$ transition). In that way, the triple-activator photoluminescence (PL) of this hybrid can be used as excellent self-referencing optical temperature thermometer. The FIR method have been carefully studied based on NTCL of the highly efficient triple-activator PL ($^5D_0$-$^7F_2$ transition of Eu^{3+} and $4f^65d$-$^8S_{7/2}$ transition of Eu^{2+}, and $^5D_0$-$^7F_2$ transition of Eu^{3+} and $^5D_4$-$^7F_5$ transition of Tb^{3+}) in a wider range (298−773 K) than most of the Eu/Tb co-doped materials.

2 Experiment

The synthesis processes of Eu/Tb/SnO_2 NCs co-doped silica glasses were described clearly in our previous works with an *in-situ* method followed by a heat treatment[27-30]. $EuCl_3 \cdot 6H_2O$ (99.99%), $TbCl_3 \cdot 6H_2O$ (99.9%), $SnCl_4 \cdot 5H_2O$ (99.995%), and deionized water were used as raw materials. Firstly, mesoporous silica glasses with mesopore size around 5−40 nm were immersed into the solutions (as listed in Tab. S1) for about 24 hours. Secondly, the doped glasses were dried in super-clean air for nearly 2 hours. Finally, the dried glasses were sintered in air to 1 000 ℃.

X-ray diffraction (XRD) patterns and micromorphology of the hybrids were collected using X'Pert PRO with Cu Kα radiation (λ=0.154 nm) at scanning speed of 10 degree per minute in the range from 10° to 70° and Tecnai G20 U-Twin Transmission Electron Microscope (TEM). LabRAM HR800 with a cooled CCD detector (He-Ne laser, 325 nm, 0.3 mW) and Edinburgh FLS980 fluorescence spectrometer were used to characterize the PL spectra and the

decay curves.

3 Results and Discussion

Fig. 1(a) and Fig. S1 show the XRD patterns of all the samples named in Tab. S1. In all the samples, the diffraction peaks at two-theta angles of 26.6°, 33.9°, 37.9°, 51.8° were clearly shown, which corresponded to the crystal planes (110), (101), (200), and (211), respectively, of the tetragonal structure SnO_2 (refer to ICDD PDF card No. 41-1445)[31-32]. The broad amorphous peak at two-theta angles 15°–25° belongs to silica glass matrix. There is no big difference in the crystal peaks with increasing concentration of Tb^{3+}. As shown in Fig. 1(b), the SnO_2 NCs in silica glass are mostly oval, with size ranging from 5–30 nm. Fig. 1(c) showed one SnO_2 NC around 15 nm and its TEM mapping images were shown in Fig. 1(d) (overlay), Fig. 1(e) (Sn), Fig. 1(f) (Eu), and Fig. 1(g) (Tb). It is clear that most of Sn was distributed in the SnO_2 NC, with little in the silica glass matrix. Eu and Tb were homogeneously distributed both in the SnO_2 NC and silica glass matrix. It indicates that more Eu and Tb were in or near the SnO_2 NC than in the glass matrix.

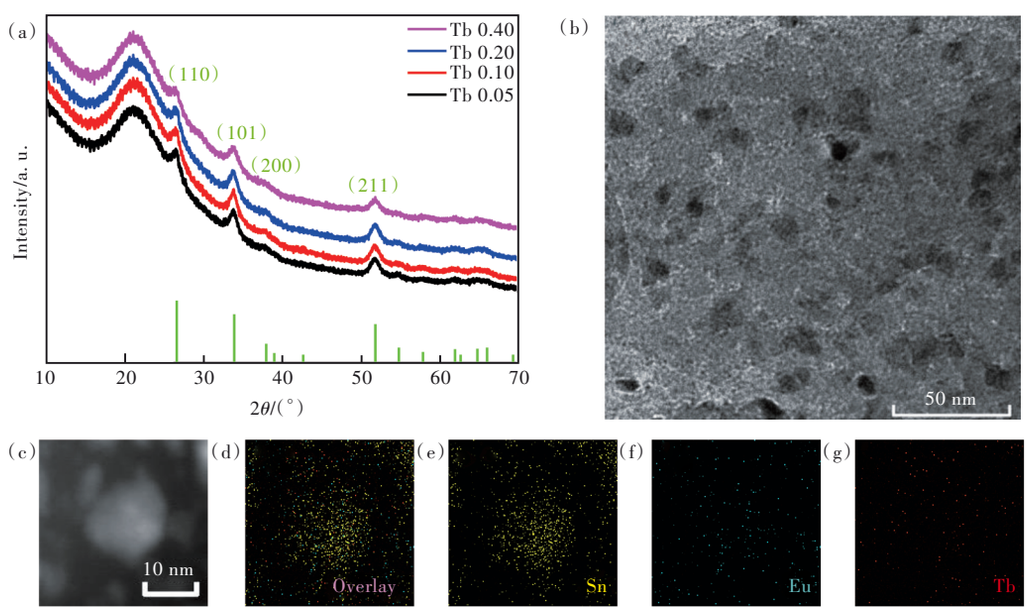

Fig. 1 (a) XRD patterns of Eu/Tb/SnO_2 NCs co-doped silica glasses with different concentration of Tb^{3+}, named Tb 0.05, Tb 0.10, Tb 0.20, and Tb 0.40, respectively. (b) TEM image of Tb 0.10. (c)–(d) TEM mapping of Tb 0.10 (three elements Sn(e), Eu(f), and Tb(g)).

As illustrated in Fig. 2(a), there are several emission peaks centered at 434, 542, 575, 588, 620 nm. The emission peaks at 434 nm and 542 nm belong to $4f^65d$-$^8S_{7/2}$ transition of Eu^{2+} and $^5D_4$-$^7F_5$ transition of Tb^{3+}, respectively. The other emission peaks all correspond to Eu^{3+}. From Fig. S2, the emission intensity at 434, 542, 575, 620 nm all increased first and then decreased with the increasing concentration of Tb^{3+}, which reached max at Tb 0.10. The emission intensities of 434, 575, 620 nm increase first because of increased sensitization centers. The emission intensities of 542 nm increase first because of increased luminescent centers. They all decrease with the doping concentration beyond the optimal concentration due to the increase of intra ionic non-radiative relaxation between adjacent RE ions[33]. The emission of Eu^{3+} is the strongest while the emission of Tb^{3+} is the weakest in all the samples. Compared to the PL emission spectra of the sample doped without Tb^{3+} in Fig. S3, one can see that the introducing of Tb^{3+} greatly enhanced the emission of Eu^{2+} and decreased the emission of Eu^{3+} at 588, 593, 598 nm corresponding to $^5D_0$-$^7F_1$ transitions. The strongest peak of Eu^{3+} in silica glasses shifts from $^5D_0$-$^7F_1$ transition to $^5D_0$-$^7F_2$ transition by adding Tb^{3+}. The relative intensities of $^5D_0$-$^7F_1$ and $^5D_0$-$^7F_2$ transitions are typical magnetic and electronic dipole transitions, respectively, which depend strongly on the

local symmetry of Eu^{3+}[34]. $^5D_0$-$^7F_1$ transition is dominating in a site with inversion symmetry. $^5D_0$-$^7F_2$ transition is the strongest in a site without inversion symmetry. Therefore, the intensities of $^5D_0$-$^7F_1$ transition change with the amount of Tb^{3+} inconsistent with the changes of the peaks at 434, 542, 575, 620 nm might result from the change of the Eu^{3+} site symmetry after co-doping with Tb^{3+}. In Fig. S4, for the sample co-doped with only Tb^{3+} and SnO_2 NCs, besides the peak at 542 nm, there is also one wide peak centered at 574 nm which belongs to the defect emission of SnO_2 NCs[28]. From Fig. 2(b), the lifetime of Eu^{2+} at 434 nm followed a similar trend as the PL emission. Compared with Fig. 2(c) and Fig. S5, the lifetime of Tb^{3+} at 542 nm almost followed a decreasing trend with the increasing concentration and the adding of Eu reduced the lifetime of Tb^{3+} from 3.282 ms to 2.755 ms. The lifetime of Eu^{3+} at 620 nm shown in Fig. 2(d) kept almost steady, which is much shorter than the sample doped without Tb^{3+} (2.197 ms)[28]. Upon the above results, there might be energy transfer from Tb^{3+} to Eu^{3+}/Eu^{2+} as shown in Fig. S6[35-37].

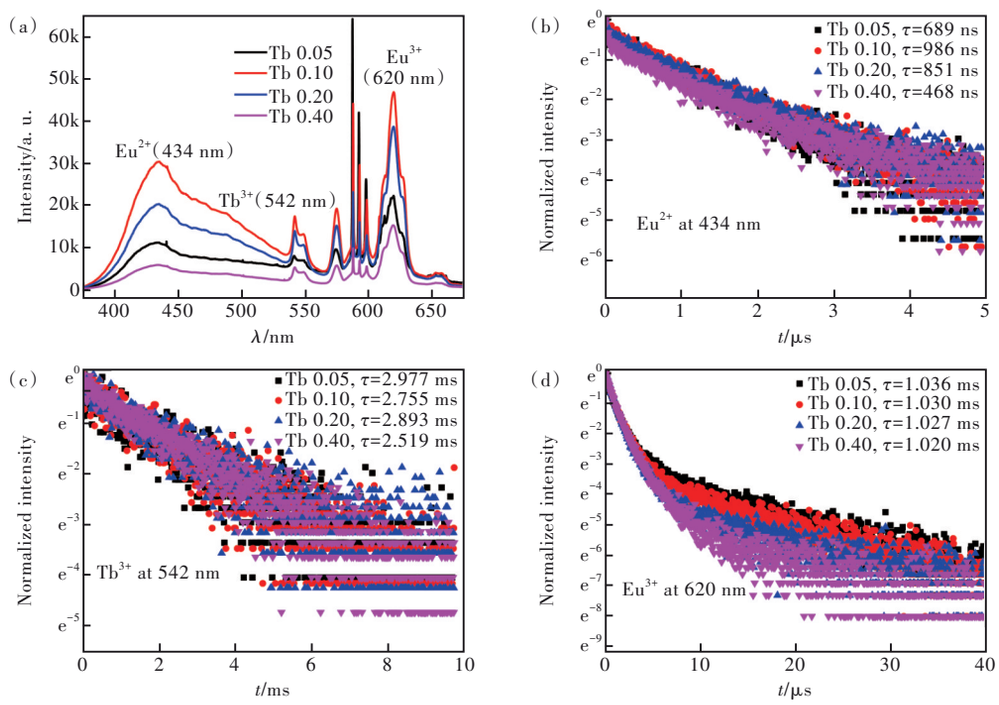

Fig.2　(a) Room temperature PL spectra of Eu/SnO_2 NCs co-doped silica glasses with different concentration of Tb^{3+} excited at 325 nm. PL decay curves of Tb 0.05, Tb 0.10, Tb 0.20, and Tb 0.40 at 434 nm(b), 542 nm(c), and 620 nm(d).

As there are three different emitters in the Eu/Tb/SnO_2 NCs co-doped silica glasses, it might be used as self-referencing luminescent thermometer with a FIR method. Therefore, the temperature-dependent PL spectra of Tb 0.10 from 298 K to 773 K were shown in Fig. 3(a). From Fig. S7, the PL intensity at 620 nm diminished quickly with the increase of temperature. The PL intensity at 542 nm also followed a decreasing trend with a much slower speed. While the PL intensity at 434 nm showed slight change in the low temperature range 298–448 K and kept a slow downward trend after 448 K. At 298 K, the intensity of Eu^{3+} is 4 times higher than that of Eu^{2+}, which shows a red colour of the glass. However, the intensity of Eu^{2+} is 22 times more intense than that of Eu^{3+} at 773 K, indicating the dominated emission has shifted from Eu^{3+} to Eu^{2+} in the high temperature range. Besides, the intensity of Tb^{3+} becomes more intense than that of Eu^{3+} after 548 K. It can be seen that Tb 0.10 can be an excellent candidate for ratiometric luminescent thermometers as the intensity shows a T-dependent behaviour and shifts in opposite directions[14]. As shown in Fig. 3(b) and Fig. 3(c), the FIR (R_{FI}) can be concluded as follows[13]:

$$R_{FI} = \frac{I_1}{I_2} = \exp(A + BT + CT^2), \qquad (1)$$

here the I_1 and I_2 are the intensity of PL peak. As a result, the relative thermal sensitivity S_r should be determined as[13]:

$$S_r = \left| \frac{1}{R_{FI}} \frac{dR_{FI}}{dT} \right| = |B + 2CT|, \quad (2)$$

the correlation coefficients (R^2) of the PL intensity ratios are 99.5% and 99.4% at I_{620}/I_{434} and I_{620}/I_{542} respectively, which indicates that the relationships are well fitted by the functions in the figures inset. The S_r is shown in Fig. 3(d), which can be used to evaluate the thermometer's performance of different materials directly and quantitatively[26, 36, 38]. The S_r values of I_{620}/I_{434} and I_{620}/I_{542} both increase linearly with temperature and the maximum S_r values are 2.3%·K^{-1} and 2.1%·K^{-1} at 773 K, respectively. The high maximum S_r values indicates Tb 0.10 is a potentially excellent luminescent thermometer among inorganic thermometers[15]. Tab. 1 shows the overview of the maximal S_r of different Eu/Tb co-doped materials, which indicates Tb 0.10 has a wider

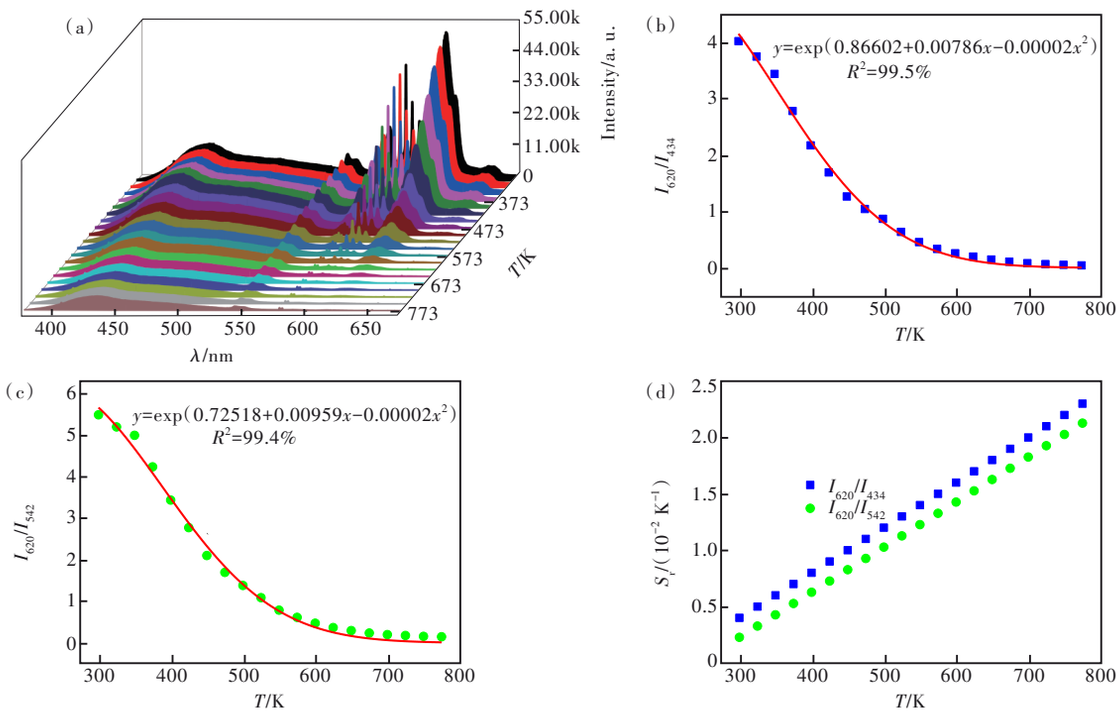

Fig.3 (a) Temperature-dependent PL spectra of the sample named Tb 0.10 excited by 325 nm. (b) PL intensity ratio of 620 nm (Eu^{3+}) to 434 nm (Eu^{2+}) and the fitted curve. (c) PL intensity ratio of 620 nm (Eu^{3+}) to 542 nm (Tb^{3+}) and the fitted curve. (d) Variation of relative sensitivity.

Tab. 1 Overview of the maximal S_r of different Eu/Tb co-doped materials

Sample	Maximal S_r/(%·K^{-1})	Temperature range/K	Reference
$Na[(Gd_{0.8}Eu_{0.1}Tb_{0.1})SiO_4]$	2.0	12–450	[39]
Eu, Tb 2D MOF sheets	1.08	110–360	[26]
$Y_2O_3:Tb^{3+},Eu^{3+}$	0.683	313–513	[40]
$Eu_{0.05}Tb_{1.95}$-PDC	1.37	293–333	[41]
MOF-5: Eu, Tb	1.8	303–473	[8]
$NaLa(MoO_4)_2:Tb^{3+},Eu^{3+}$	1.42	293–593	[42]
$Eu_{0.0316}Tb_{0.9684}$BTPTA	5.12	25–225	[43]
$Eu_{0.37}Tb_{0.63}$-BTC-a	0.68	313–473	[44]
$SrF_2:Tb^{3+},Eu^{3+}$		298–473	[45]
$CaMoO_4$: 5%Tb^{3+}, 0.3% Eu^{3+}	1.18	298–603	[25]
$Sc_2O_3:Eu^{2+}/Eu^{3+}/Tb^{3+}$	2.65	137–267	[13]
Silica glass: $Eu^{2+}/Eu^{3+}/Tb^{3+}/SnO_2$	2.3	298–773	This work

probing range and higher S_r than most Eu/Tb co-doped materials.

Repeatability is a vital parameter for sensor[13,17]. As shown in Fig. 4, the repeatability is 93.90% for I_{620}/I_{434} and 95.18% for I_{620}/I_{542}, which was obtained by heating-cooling four cycles. This suggests Tb 0.10 has good repeatability as luminescent thermometers.

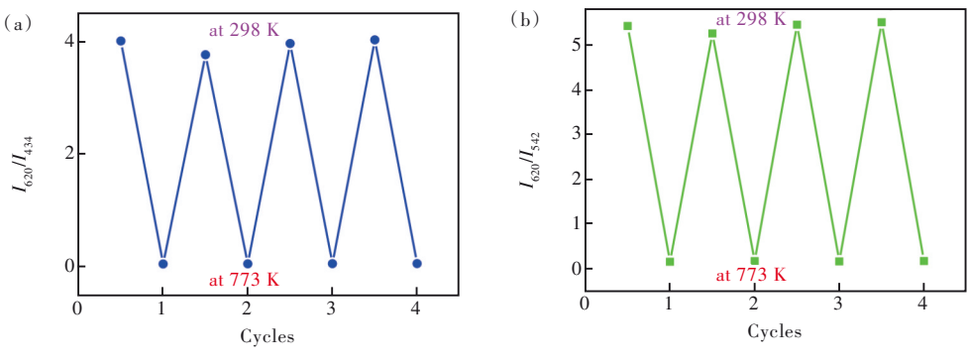

Fig.4　Four cycles of intensity ratio variations measured at 298 K and 773 K of I_{620}/I_{434}(a) and I_{620}/I_{542}(b)

4　Conclusion

In summary, we report the triple-emitting photoluminescence of Eu/Tb/SnO_2 NCs co-doped silica glasses for self-referencing temperature probing. The temperature dependent FIR of Eu^{3+}/Eu^{2+} and Eu^{3+}/Tb^{3+} were used for measuring temperature in a wide range of 298–773 K. The S_r values of I_{620}/I_{434} and I_{620}/I_{542} both increase linearly with temperature and the maximum S_r values are 2.3%·K^{-1} and 2.1%·K^{-1} at 773 K, respectively. The S_r values are higher than most Eu/Tb co-doped materials, which indicates the potential of this hybrid in self-referencing optical temperature measurement with triple activators.

Supplementary Information and Response Letter are available for this paper at: http://cjl.lightpublishing.cn/thesisDetails#10.37188/CJL.20230212.

References:

[1] ZHANG F Z, WANG F X, LI Y, *et al.* Real-time cell temperature fluctuation monitoring system using precision Pt sensors coated with low thermal capacity, low thermal resistance, and self-assembled multilayer films [J]. *ACS Sens.*, 2023, 8(1): 141-149.

[2] SONG E H, CHEN M H, CHEN Z T, *et al.* Mn^{2+}-activated dual-wavelength emitting materials toward wearable optical fibre temperature sensor [J]. *Nat. Commun.*, 2022, 13(1): 2166.

[3] MORAD V, YAKUNIN S, BENIN B M, *et al.* Hybrid 0D antimony halides as air-stable luminophores for high-spatial-resolution remote thermography [J]. *Adv. Mater.*, 2021, 33(9): 2007355.

[4] CHEN R, LUO T, GENG D, *et al.* Facile fabrication of a fast-response flexible temperature sensor *via* laser reduced graphene oxide for contactless human-machine interface [J]. *Carbon*, 2022, 187: 35-46.

[5] CHEN P, XU X, LI D Y, *et al.* 2D van der Waals rare earth material based ratiometric luminescence thermography integrated on micro-nano devices vertically [J]. *Adv. Opt. Mater.*, 2022, 10(6): 2102102.

[6] SUO H, ZHAO X Q, ZHANG Z Y, *et al.* Rational design of ratiometric luminescence thermometry based on thermally coupled levels for bioapplications [J]. *Laser Photonics Rev.*, 2021, 15(1): 2000319.

[7] CHEN C J, ZHUANG Y X, LI X Y, *et al.* Achieving remote stress and temperature dual-modal imaging by double-lanthanide-activated mechanoluminescent materials [J]. *Adv. Funct. Mater.*, 2021, 31(25): 2101567.

[8] XIA C, YU C Y, CAO M M, *et al.* A Eu and Tb co-doped MOF-5 compound for ratiometric high temperature sensing [J]. *Ceram. Int.*, 2018, 44(17): 21040-21046.

[9] WANG Z Y, JIAO H, FU Z L. Investigation on the up-conversion luminescence and temperature sensing properties based on non-thermally coupled levels of rare earth ions doped $Ba_2In_2O_5$ phosphor [J]. *J. Lumin.*, 2019, 206: 273-277.

[10] LIU J, VAN DEUN R, KACZMAREK A M. Optical thermometry of MoS_2:Eu^{3+} 2D luminescent nanosheets [J]. *J. Mater. Chem.* C, 2016, 4(42): 9937-9941.

[11] SENAPATI S, NANDA K K. Red emitting Eu:ZnO nanorods for highly sensitive fluorescence intensity ratio based optical thermometry [J]. *J. Mater. Chem.* C, 2017, 5(5): 1074-1082.

[12] FENG J F, LIU T F, SHI J L, *et al*. Dual-emitting UiO-66(Zr&Eu) metal-organic framework films for ratiometric temperature sensing [J]. *ACS Appl. Mater. Interfaces*, 2018, 10(24): 20854-20861.

[13] PAN Y, XIE X J, HUANG Q W, *et al*. Inherently Eu^{2+}/Eu^{3+} codoped Sc_2O_3 nanoparticles as high-performance nanothermometers [J]. *Adv. Mater.*, 2018, 30(14): 1705256.

[14] PENG X W, LIU Q Y, WANG H H, *et al*. Eu(Ⅲ)- and Tb(Ⅲ)-coordination polymer luminescent thermometers constructed from a π-rich aromatic ligand exhibiting a high sensitivity [J]. *Dyes Pigm.*, 2019, 162: 405-411.

[15] NIKOLIĆ M G, ANTIĆ Ž, ĆULUBRK S, *et al*. Temperature sensing with Eu^{3+} doped TiO_2 nanoparticles [J]. *Sens. Actuators* B: *Chem.*, 2014, 201: 46-50.

[16] CHEN D Q, LIU S, ZHOU Y, *et al*. Dual-activator luminescence of *RE*/*TM*:$Y_3Al_5O_{12}$ (*RE* = Eu^{3+}, Tb^{3+}, Dy^{3+}; *TM* = Mn^{4+}, Cr^{3+}) phosphors for self-referencing optical thermometry [J]. *J. Mater. Chem.* C, 2016, 4(38): 9044-9051.

[17] WANG C Y, LIN H, XIANG X Q, *et al*. $CsPbBr_3$/$EuPO_4$ dual-phase devitrified glass for highly sensitive self-calibrating optical thermometry [J]. *J. Mater. Chem.* C, 2018, 6(37): 9964-9971.

[18] ZHENG S H, CHEN W B, TAN D Z, *et al*. Lanthanide-doped $NaGdF_4$ core-shell nanoparticles for non-contact self-referencing temperature sensors [J]. *Nanoscale*, 2014, 6(11): 5675-5679.

[19] CHEN G R, LEI R S, HUANG F F, *et al*. Optical temperature sensing behavior of Er^{3+}/Yb^{3+}/Tm^{3+}:Y_2O_3 nanoparticles based on thermally and non-thermally coupled levels [J]. *Opt. Commun.*, 2018, 407: 57-62.

[20] CHEN G R, LEI R S, WANG H P, *et al*. Temperature-dependent emission color and temperature sensing behavior in Tm^{3+}/Yb^{3+}:Y_2O_3 nanoparticles [J]. *Opt. Mater.*, 2018, 77: 233-239.

[21] GAO Y, HUANG F, LIN H, *et al*. A novel optical thermometry strategy based on diverse thermal response from two intervalence charge transfer states [J]. *Adv. Funct. Mater.*, 2016, 26(18): 3139-3145.

[22] HAN Q, HAO H Y, YANG J S, *et al*. Optical temperature sensing based on thermal, non-thermal coupled levels and tunable luminescent emission colors of Er^{3+}/Tm^{3+}/Yb^{3+} tri-doped $Y_7O_6F_9$ phosphor [J]. *J. Alloys Compd.*, 2019, 786: 770-778.

[23] LU H Y, HAO H Y, GAO Y C, *et al*. Optical sensing of temperature based on non-thermally coupled levels and upconverted white light emission of a $Gd_2(WO_4)_3$ phosphor co-doped with in Ho(Ⅲ), Tm(Ⅲ), and Yb(Ⅲ) [J]. *Microchim. Acta*, 2017, 184(2): 641-646.

[24] ZHAO D, YUE D, ZHANG L, *et al*. Cryogenic luminescent Tb/Eu-MOF thermometer based on a fluorine-modified tetracarboxylate ligand [J]. *Inorg. Chem.*, 2018, 57(20): 12596-12602.

[25] LI S D, MENG Q Y, LÜ S C, *et al*. Study on optical temperature sensing properties of Tb^{3+}, Eu^{3+} co-doped $CaMoO_4$ phosphor [J]. *J. Lumin.*, 2018, 200: 103-110.

[26] KACZMAREK A M. Eu^{3+}/Tb^{3+} and Dy^{3+} POM@MOFs and 2D coordination polymers based on pyridine-2, 6-dicarboxylic acid for ratiometric optical temperature sensing [J]. *J. Mater. Chem.* C, 2018, 6(22): 5916-5925.

[27] CHEN P, MAO Y W, HOU S D, *et al*. Effects of In_2O_3 nanoparticles doping on the photoluminescent properties of Eu^{2+}/Eu^{3+} ions in silica glasses [J]. *Ceram. Int.*, 2019, 45(1): 233-238.

[28] CHEN P, MAO Y W, HOU S D, *et al*. Growth of SnO_2 nanocrystals co-doped with Eu^{3+} for highly enhanced photoluminescence in mesoporous silica glasses [J]. *J. Mater. Chem.* C, 2019, 7(6): 1568-1574.

[29] CHEN P, CHEN Z R, HOU S D, *et al*. *In-situ* growth of highly monodisperse ITO nanoparticles regulated by mesoporous silica glasses [J]. *Mater. Des.*, 2018, 151: 53-59.

[30] CHEN P, HOU S D, YANG Y, *et al*. ITO nanoparticles enhanced upconversion luminescence in Er^{3+}/Yb^{3+}-codoped silica glasses [J]. *Nanoscale*, 2018, 10(7): 3299-3306.

[31] DAS S, JAYARAMAN V. SnO_2: a comprehensive review on structures and gas sensors [J]. *Prog. Mater. Sci.*, 2014, 66: 112-255.

[32] STRAUSS M, DESTEFANI T A, SIGOLI F A, *et al*. Crystalline SnO_2 nanoparticles size probed by Eu^{3+} luminescence [J]. *Cryst. Growth Des.*, 2011, 11(10): 4511-4516.

[33] 崔祥水, 陈文哲. 稀土离子(Eu^{3+}, Tb^{3+}, Ce^{3+})掺杂$ZnAl_2O_4/SiO_2$微晶玻璃的制备与发光性能[J]. 发光学报, 2015, 36(4): 400-407.
CUI X S, CHEN W Z. Preparation and luminescence properties of $ZnAl_2O_4/SiO_2$:RE^{3+} (*RE* = Eu, Tb, Ce) glass ceramics by sol-gel method [J]. *Chin. J. Lumin.*, 2015, 36(4): 400-407. (in English)

[34] 石冬梅, 赵营刚. Eu/Tm/Tb掺杂硼硅酸盐玻璃的发光性能[J]. 发光学报, 2016, 37(4): 392-398.
SHI D M, ZHAO Y G. Luminescence properties of Eu/Tm/Tb-doped borosilicate glass [J]. *Chin. J. Lumin.*, 2016, 37(4): 392-398. (in Chinese)

[35] CHENG Y, GAO Y, LIN H, *et al.* Strategy design for ratiometric luminescence thermometry: circumventing the limitation of thermally coupled levels [J]. *J. Mater. Chem.* C, 2018, 6(28): 7462-7478.

[36] MARCINIAK L, BEDNARKIEWICZ A. The influence of dopant concentration on temperature dependent emission spectra in $LiLa_{1-x-y}Eu_xTb_yP_4O_{12}$ nanocrystals: toward rational design of highly-sensitive luminescent nanothermometers [J]. *Phys. Chem. Chem. Phys.*, 2016, 18(23): 15584-15592.

[37] GOPI S, JOSE S K, SREEJA E, *et al.* Tunable green to red emission *via* Tb sensitized energy transfer in Tb/Eu co-doped alkali fluoroborate glass [J]. *J. Lumin.*, 2017, 192: 1288-1294.

[38] MARCINIAK L, BEDNARKIEWICZ A, KOWALSKA D, *et al.* A new generation of highly sensitive luminescent thermometers operating in the optical window of biological tissues [J]. *J. Mater. Chem.* C, 2016, 4(24): 5559-5563.

[39] ANANIAS D, PAZ F A A, YUFIT D S, *et al.* Photoluminescent thermometer based on a phase-transition lanthanide silicate with unusual structural disorder [J]. *J. Am. Chem. Soc.*, 2015, 137(8): 3051-3058.

[40] PENG L X, MENG Q Y, SUN W J. Size dependent optical temperature sensing properties of Y_2O_3:Tb^{3+}, Eu^{3+} nanophosphors [J]. *RSC Adv.*, 2019, 9(5): 2581-2590.

[41] ZHOU X, WANG H W, JIANG S, *et al.* Multifunctional luminescent material Eu(Ⅲ) and Tb(Ⅲ) complexes with pyridine-3,5-dicarboxylic acid linker: crystal structures, tunable emission, energy transfer, and temperature sensing [J]. *Inorg. Chem.*, 2019, 58(6): 3780-3788.

[42] PENG L X, MENG Q Y, SUN W J. Synthesis and optical temperature sensing performance of $NaLa(MoO_4)_2$:Tb^{3+}, Eu^{3+} phosphors [J]. *Ceram. Int.*, 2019, 45(16): 20656-20663.

[43] ZHU Y Y, XIA T F, ZHANG Q, *et al.* A Eu/Tb mixed lanthanide coordination polymer with rare 2D thick layers: synthesis, characterization and ratiometric temperature sensing [J]. *J. Solid State Chem.*, 2018, 259: 98-103.

[44] WANG H Z, ZHAO D, CUI Y A J, *et al.* A Eu/Tb-mixed MOF for luminescent high-temperature sensing [J]. *J. Solid State Chem.*, 2017, 246: 341-345.

[45] YAN Y, TAN Y J, LI D W, *et al.* Efficient energy transfer, multi-colour emitting and temperature sensing behavior of single-phase Tb^{3+}, Eu^{3+} co-doped strontium fluoride phosphors [J]. *J. Lumin.*, 2019, 211: 209-217.

陈萍(1992-),女,安徽桐城人,博士,副教授,2019年于华中科技大学获得博士学位,主要从事稀土发光材料方面的研究。
E-mail: chenp@hfut.edu.cn

戴能利(1970-),男,重庆人,博士,教授,2004年于中国科学院上海光学精密机械研究所获得博士学位,主要从事新型光纤材料、光纤激光和光学测试技术的研究。
E-mail: dainl@mail.hust.edu.cn